Jacot E, van den Abbeele T, Debre HR, Wiener-Vacher SR: Vestibular impairments pre- and post-cochlear implant in children. Int J Pediatr Otorhinolaryngol 2009;73:209–217.
Jin Y, Nakamura M, Shinjo Y, Kaga K: Vestibular-evoked myogenic potentials in cochlear implant children. Acta Otolaryngol 2006;126:164–169.
Kaga K: Vestibular compensation in infants and children with congenital and acquired vestibular loss in both ears. Int J Pediatr Otorhinolaryngol 1999;49:215–224.
Kaga K, Shinjo Y, Jin Y, Takegoshi H: Vestibular failure in children with congenital deafness. Int J Audiol 2008;47:590–599.
Kaga K, Suzuki JI, Marsh RR, Tanaka Y: Influence of labyrinthine hypoactivity on gross motor development of infants. Ann NY Acad Sci 1981;374:412–420.
Kelsch TA, Schaefer LA, Esquivel CR: Vestibular evoked myogenic potentials in young children: test parameters and normative data. Laryngoscope 2006;116:895–900.
McCue MP, Guinan JJ: Acoustically responsive fibers in the vestibular nerve of the cat. J Neurosci 1994;14:6058–6070.
Murofushi T, Curthoys IS, Topple AN, Colebatch JG, Halmagyi GM: Responses of guinea pig primary vestibular neurons to clicks. Exp Brain Res 1995;103:174–178.
Murofushi T, Halmagyi GM, Yavor RA, Colebatch JG: Absent vestibular evoked myogenic potentials in vestibular neurolabyrinthitis. An indicator of inferior vestibular nerve involvement? Arch Otolaryngol Head Neck Surg 1996;122:845–848.
Murofushi T, Matsuzaki M, Mizuno M: Vestibular evoked myogenic potentials in patients with acoustic neuromas. Arch Otolaryngol Head Neck Surg 1998;124:509–512.
Murofushi T, Matsuzaki M, Wu CH: Short tone burst-evoked myogenic potentials on the sternocleidomastoid muscle: are these potentials also of vestibular origin? Arch Otolaryngol Head Neck Surg 1999;125:660–664.
Potter CN, Silverman LN: Characteristics of vestibular function and static balance skills in deaf children. Phys Ther 1984;64:1071–1075.
Rine RM, Cornwall G, Gan K, LoCascio C, O'Hare T, Robinson E, Rice M: Evidence of progressive delay of motor development in children with sensorineural hearing loss and concurrent vestibular dysfunction. Percept Mot Skills 2000;90:1101–1112.
Sennaroglu L, Saatci I: A new classification for cochleovestibular malformations. Laryngoscope 2002;112:2230–2241.
Sheykholeslami K, Megerian CA, Arnold JE, Kaga K: Vestibular-evoked myogenic potentials in infancy and early childhood. Laryngoscope 2005;115:1440–1444.
Shinjo Y, Jin Y, Kaga K: Assessment of vestibular function of infants and children with congenital and acquired deafness using the ice-water caloric test, rotational chair test and vestibular-evoked myogenic potential recording. Acta Otolaryngol 2007;127:736–747.
Suarez H, Angeli S, Suarez A, Rosales B, Carrera X, Alonso R: Balance sensory organization in children with profound hearing loss and cochlear implants. Int J Pediatr Otorhinolaryngol 2007;71:629–637.
Todt I, Hennies HC, Basta D, Ernst A: Vestibular dysfunction of patients with mutations of connexin 26. Neuroreport 2005;16:1179–1181.
Tribukait A, Brantberg K, Bergenius J: Function of semicircular canals, utricle and saccules in deaf children. Acta Otolaryngol 2004;124:41–48.
Tsukada K, Nishio S, Usami S, Deafness Gene Study Consortium: A large cohort study of *GJB2* mutations in Japanese hearing loss patients. Clin Genet 2010;78:464–470.
Viciana D, Lopez-Escamez JA: Short tone bursts are better than clicks for cervical vestibular-evoked myogenic potentials in clinical practice. Eur Arch Otorhinolaryngol 2012;269:1857–1863.
Wallacott MH, Assaiante C, Amblard B: Development of balance and gait control; in Bronstein AM, Brandt T, Wallacott MH, Nutt JG (eds): Clinical Disorders of Balance, Posture and Gait, ed 2. London, Arnold, 2004, pp 39–62.
Welgampola MS, Colebatch JG: Characteristics and clinical applications of vestibular-evoked myogenic potentials. Neurology 2005;64:1682–1688.
Zagólski O: Vestibular-evoked myogenic potentials and caloric stimulation in infants with congenital cytomegalovirus infection. J Laryngol Otol 2008;122:574–579.

Auris Nasus Larynx 40 (2013) 510–513

Contents lists available at SciVerse ScienceDirect

Auris Nasus Larynx

journal homepage: www.elsevier.com/locate/anl

Cochlear implantation in a patient with osteogenesis imperfecta

Yoshimi Makizumi, Akinori Kashio, Takashi Sakamoto, Shotaro Karino, Akinobu Kakigi, Shinichi Iwasaki, Tatsuya Yamasoba *

Department of Otolaryngology and Head and Neck Surgery, Graduate School of Medicine, The University of Tokyo, Japan

ARTICLE INFO

Article history:
Received 18 May 2012
Accepted 9 November 2012
Available online 6 December 2012

Keywords:
Cochlear implantation
Osteogenesis imperfecta
Facial nerve stimulation

ABSTRACT

Osteogenesis imperfecta (OI) is a connective tissue disorder characterized by a deficit in the synthesis of type I collagen. Hearing loss affects 42–58% of OI patients and progresses to deafness in 35–60% of these patients. For OI patients, cochlear implantation (CI) is the only promising treatment option. However, literature on CI in patients with OI is relatively rare. After CI, speech perception is generally good. However, among patients with severe demineralization of the cochlea, most patients are reported to have complications of facial nerve stimulation (FNS), preventing some patients from using the cochlear implant on a daily basis. Here we report a successful CI using a Nucleus CI24 Contour Advance cochlear implant in a patient with OI. Although high-resolution computed tomography (HRCT) showed extensive demineralization of the cochlea, intracochlear electrodes were inserted properly. The use of a modiolus-hugging device and the advance off-stylet technique contributed to the successful implantation, with no complications such as FNS or misplacement of electrodes. Therefore, CI can be used for treating deaf patients with OI.

1. Introduction

Osteogenesis imperfecta (OI) is a connective tissue disorder characterized by a deficit in the synthesis of type I collagen [1]. OI was first described by van der Hoeve and de Kleyn in 1917 [2] and, therefore, is also known as van der Hoeve–de Kleyn syndrome. The disease is characterized by brittle bones, blue sclerae, defective dentition and hearing loss [3]. Progressive hearing loss has been reported, including conductive, sensorineural, or mixed types [4]. Conductive hearing loss may be the result of a fracture or localized dehiscence of the stapedial arch, distal atrophy of the long process of the incus, or fixation of the stapedial footplate [1]. Sensorineural hearing loss is caused by microfractures, hemorrhage, and encroachment of reparative vascular and fibrous tissue in and around the cochlea [1]. Previous studies have reported hearing loss in 42–58% of OI patients and profound deafness in 35–60% of OI patients [5–9]. Hearing loss usually begins in the late teens in OI patients. The sensorineural component appears and progresses gradually in the third decade, resulting in profound deafness by the end of the fourth to fifth decade [7]. Cochlear implantation (CI) is the only treatment option for profound sensorineural hearing loss. However, the scientific and medical literature on CI in patients with OI is relatively rare [5–10]. After CI, speech perception is generally good. However, most patients with severe demineralization of the cochlea are reported to have complications of facial nerve stimulation (FNS). Several cases of electrode mis-insertion have also been reported. Some patients with such complications give up daily use of the cochlear implant [7,11].

Here, we report a successful CI using a Nucleus CI24 Contour Advance (CA) cochlear implant in a patient with OI. Although high-resolution computed tomography (HRCT) showed extensive demineralization of the cochlea, intracochlear electrodes were properly inserted without any of the common complications.

2. Case presentation

A female patient had several episodes of bone fractures due to minor trauma from childhood. At 18-years of age, she began to complain of bilateral hearing loss. A clinical examination revealed blue sclerae with hearing loss, and the patient was diagnosed as OI based on the clinical criteria [12] at the age of 21 years. The patient had no family history of OI or hearing loss, except for her grandfather who had presbycusis. At the age of 27 years, the patient underwent an ossiculoplasty of the left ear that unfortunately resulted in deafness. Subsequently, she began to wear a hearing aid in the right ear. At the age of 52 years, the patient consulted our department when her hearing acuity in the right ear worsened. An otoscopy examination revealed normal tympanic membranes in both ears. A pure-tone audiogram demonstrated

* Corresponding author at: Department of Otolaryngology and Head and Neck Surgery, Faculty of Medicine, The University of Tokyo, Hongo 7-3-1, Bunkyo-ku, Tokyo 113-8655, Japan. Tel.: +81 3 5800 8924; fax: +81 3 3814 9486.
E-mail address: tyamasoba-tky@umin.ac.jp (T. Yamasoba).

0385-8146/$ – see front matter © 2012 Elsevier Ireland Ltd. All rights reserved.
http://dx.doi.org/10.1016/j.anl.2012.10.006

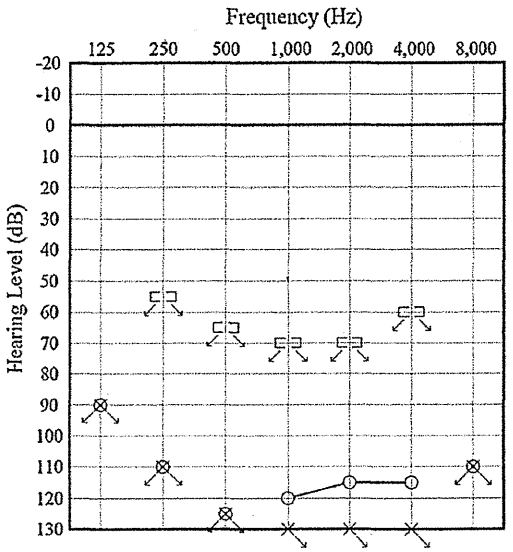

Fig. 1. Preoperative audiogram. A pure-tone audiogram demonstrated profound sensorineural hearing loss in both ears.

profound sensorineural hearing loss in both ears (Fig. 1). A speech discrimination test revealed no identification ability in both ears. Speech recognition scores with a hearing aid showed that only 10% of phonemes were recognized in the open set condition and 24% were recognized with verbal cues. The vestibular evoked myogenic potential (VEMP) was absent in both sides. A caloric test did not evoke nystagmus in either ear. A promontory stimulation test produced good auditory perception in both ears. HRCT revealed severe demineralization of the pericochlear and vestibular areas in both sides, and the outline of the cochlea was almost unrecognizable (Fig. 2). Magnetic resonance imaging (MRI) showed fluid intensity in the entire cavity of the right cochlea. However, fluid intensity in the scala tympani of the basal turn was decreased in the left cochlea (Fig. 3). The right and left cochlear nerves were well recognized on MRI.

Because there was a long period of auditory deprivation of the left ear and the MRI suggested partial occlusion in the basal turn, we decided to perform CI for the right ear. At the age of 54 years, the patient underwent surgery in the right ear to implant the Nucleus CI24R Contour Advance device. A mastoidectomy and a posterior tympanotomy were performed uneventfully. The foramen obturatum and the oval window were obliterated, and the round window was barely identified by the new bone formation of the promontory. We performed *chocleostomy* using the location of stapes as a landmark. The bone of the cochlear capsule was spongiotic and fragile; however, a cochleostomy was easily performed and the scala tympani was identified. All of the 22 electrodes were inserted successfully using the advanced off-stylet (AOS) technique. Postoperative neural response telemetry (NRT) showed good responses in all electrodes without FNS. Postoperative radiography and HRCT revealed the fully inserted electrodes inside the cochlea (Fig. 4). All of the electrodes showed normal impedance at first stimulation, and

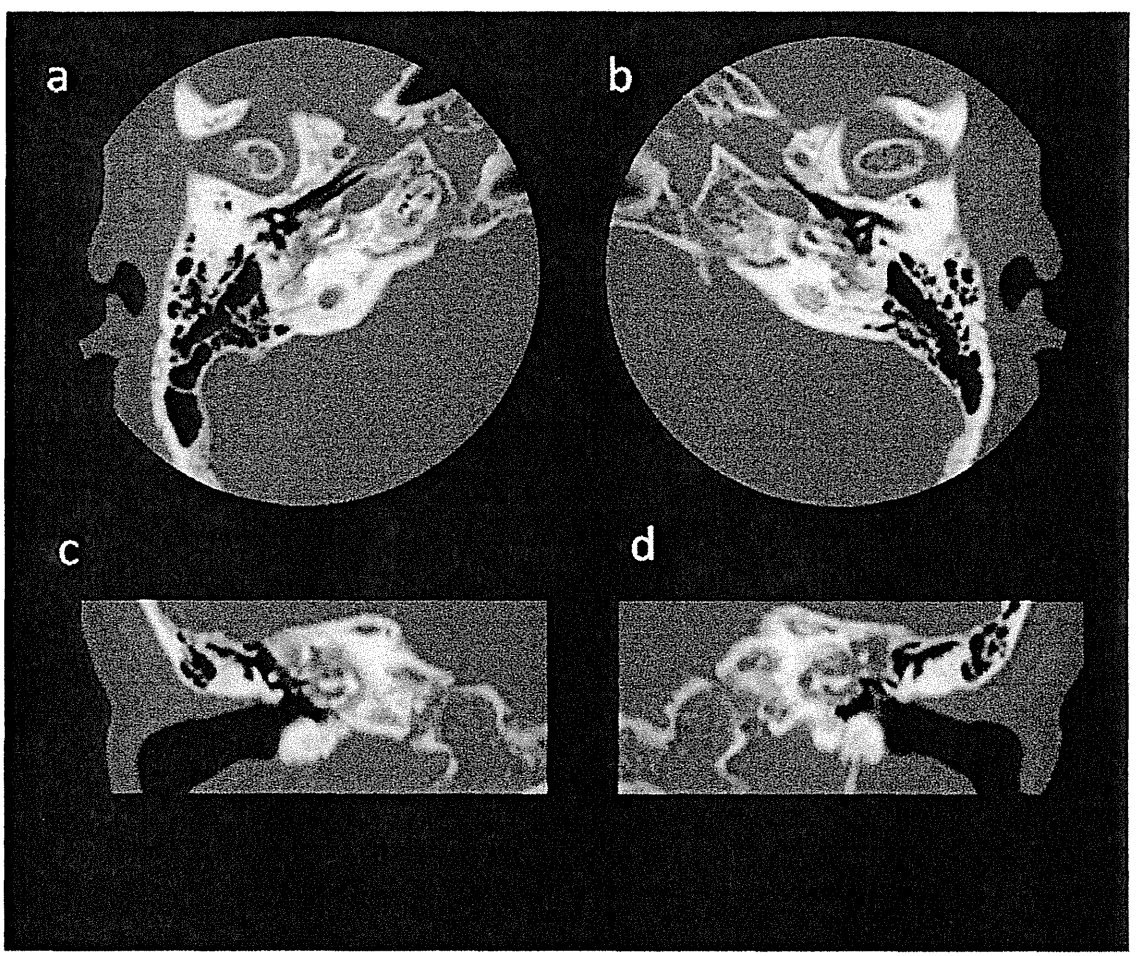

Fig. 2. Preoperative CT image of the cochlea. High resolution computed tomography (HRCT) revealed significant demineralization of the right and left pericochlear and vestibular areas, and the structures of the cochleae were almost unrecognizable.

Fig. 3. Preoperative MRI image of the cochlea. MRI demonstrated fluid content in the entire right cochlea. However, in the left cochlea, the fluid content in the scala tympani of the basal turn showed a defect, which suggested a partial occlusion.

no FNS was found during the stimulation. At the 6-month postoperative evaluation, the perception scores of monosyllables, words, and sentences using the CI and without any other cues were 62%, 70%, and 91%, respectively. These results indicated that the patient had good speech perception.

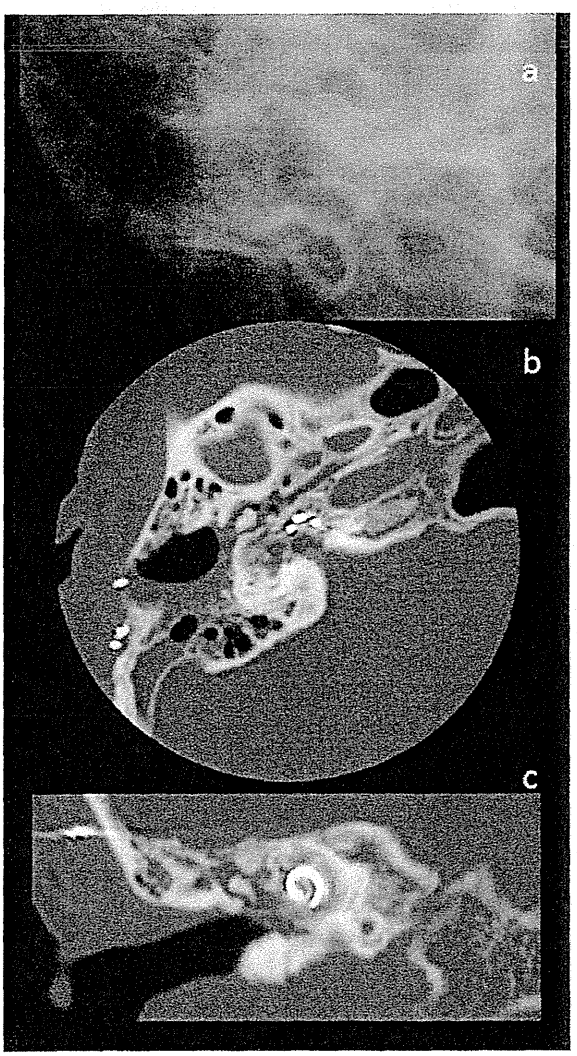

Fig. 4. Intraoperative radiograph and postoperative HRCT images of the cochlea. Intraoperative radiograph (a) and postoperative HRCT images (b and c) showed fully inserted electrodes.

3. Discussion

We have reported the case of an OI patient with a severely demineralized cochlea who underwent a successful operation for CI, resulting in good speech perception. No complications such as FNS and misplacement of electrodes were observed following the operation.

OI is a heterogeneous disease of the connective tissue caused by defective genes (*COL1A1* and *COL1A2*). *COL1A1* and *COL1A2* are responsible for the production of collagen type I, and mutations lead to defects in the bone matrix and connective tissue [7]. Recent studies have shown that reduced bone mineral density as a feature of OI and examining bone mineral density using the devices such as X-ray absorptiometry and peripheral quanitative computed tomography as well as genetic screening are becoming another powerful tool for the diagnosis of OI [13]. In this case, however, we made the diagnosis of OI based on the traditional criteria introduced by Sillence et al. [12]. Previous studies have reported various results for the prevalence of OI, ranging from 1/10,000 to 1/30,000 [6,14]. It has been reported that 2–35% of OI patients progress to deafness, with CI being the only promising treatment option [7–9]. To date, only 10 cases of CI with OI have been reported, including the present case. The HRCT findings of OI are as follows: (1) extensive dematerialized bone involving all or part of the otic capsule and extending as high as the upper margin of the superior semicircular canal; (2) fenestral manifestations caused by proliferation of bone, such as a narrow middle ear cavity, an enveloped stapes footplate, and obliterated windows with irregular and indistinct margins; and (3) involvement of the facial nerve canal in the dysplastic process [15]. These clear findings can lead surgeons to underestimate the remaining cochlear structure and space for electrodes thus improperly limiting the scope of CI. This may be the reason for the relatively small number of CIs reported for OI. In the present case, HRCT demonstrated extensive demineralization of the bony labyrinth, and the structure of cochlea was barely distinguishable. In contrast, a T2-weighted fast spin-echo (3D-FSE) MRI revealed a distinct fluid signal in the right cochlea. Based on this additional information provided by the MRI, we confidently decided to carry out CI.

In the present case, MRI showed a partial occlusion of the basal turn in the left ear. The previous ossiculoplasty might have elicited the occlusion, but we cannot deny the possibility that this occlusion was the result of ossification due to OI. Occlusion of the cochlea has also been reported in patients with otosclerosis, who have shown a similar proliferation of bones around the cochlea [16]. The genetic association with COL1A1 has been reported also in otosclerosis. Chen et al. suggested that otosclerosis has an association with single nucleotide polymorphisms in the regulatory regions of COL1A1, whereas OI is caused by a reduction in total COL1A1 mRNA secondary to mutations in COL1A1 [17]. It is possible that the association with COL1A1 in both of two diseases may cause the similar demineralization of the cochlea and that the difference in the mechanisms of COL1A1 disorder may determine the characteristics of each disease. As the present report shows, the condition of the cochlea should be carefully examined preoperatively by both HRCT and MRI. Otherwise, an evaluation by CT alone may lead to a misunderstanding of the operative indication for CI.

Because of severe demineralization of the otic capsule, CI in OI is challenging and is often accompanied by several complications. One such complication is FNS, and another is the misplacement of electrodes. Six patients with severe demineralization of the otic capsule have been reported to experience FNS as a complication after CI [5–8]. Most of the patients continued using the implant after switching off several

electrodes that caused the FNS. However, 2 patients discontinued use of the cochlear implant due to severe discomfort. It has been postulated that FNS is induced by deviant current spread throughout dehiscent or otospongiotic bone, where impedance is low, resulting in an electrical field in the proximity of the facial nerve [18]. Perimodiolar electrodes of the Nucleus CI24R CA device are tightly shielded against the lateral spread of current and theoretically are less likely to elicit FNS [19]. A CI study of patients with otosclerosis who had histopathologically similar demineralization of the cochlea showed a higher incidence (44%) of FNS in patients implanted with non modiolus-hugging devices than in those implanted with modiolus-hugging devices (10%) [20]. In the present case, no FNS occurred despite severe demineralization of the otic capsule. This is the first report of a successful CI with a perimodiolar designed electrode in an OI patient with severe demineralization of the cochlea. Additional cases are needed to establish the efficacy of the perimodiolar electrode for preventing FNS. However, perimodiolar designed electrodes may be preferable for OI patients to prevent FNS complications.

Another significant complication of CI in OI patients is misplacement of the electrodes. Two cases of misplacement have been reported. The risk of misplacement of the electrode array in a spongiotic otic capsule has also been described in patients with otosclerosis [20]. Cochlear otosclerosis is similar to OI because otospongiotic changes of the otic capsule and abnormal bone proliferation around a promontory of the otic capsule are observed in both conditions. In an OI patient, it is difficult to identify the round window niche or oval window [5]. Therefore, cochleostomy is challenging due to a lack of anatomical landmarks. Even when cochleostomy is performed in the proper place, the electrode can easily destroy the capsule and penetrate into the surrounding structures during insertion due to the soft and brittle nature of the cochlear bone. Recently, CI devices have been developed to minimize insertion trauma. The CA electrode may be used as an alternative to the traditional straight electrode, applying the AOS insertion technique so that the electrode does not touch the outer wall of the cochlea, thus reducing the risk of trauma to the cochlea [21]. With this technique, the slower insertion speed of the electrodes is also reported to impact the insertion force and reduce the risk of trauma [22]. Therefore, using this new, less traumatic device with a slower electrode insertion speed can prevent misplacement.

Our patient could recognize of 62% of phonemes, 70% of words, and 91% of sentences. Therefore, we concluded that the CI was successful. Berger et al. [23] reviewed the histopathology of the temporal bone in OI and suggested that progressive sensorineural hearing loss results from hemorrhage into the inner ear spaces. Subsequently, the accumulated cells and plasma proteins may disturb the inner ear dynamics and alter the electrolyte gradients. In this pathological condition, the spiral ganglion cells are assumed to be well preserved; therefore, good performance can be expected after CI. Nevertheless, 3 patients had an unsuccessful result in previous report. Two of these unsuccessful results were attributed to misplacement of the electrodes and severe FNS [7]. Another case involved a 6-year-old child who had profound sensorineural hearing loss from 6 months of age [8]. The poor result observed in this case can be attributed to the late age of implantation. These results show that if the electrodes are inserted properly within the appropriate period, sufficient speech perception can be expected and that CI surgery is a promising choice of treatment for OI.

4. Conclusion

We reported the case of an OI patient showing severe demineralization of the cochlea on HRCT. Preoperative MRI showed sufficient space for the CI in the basal turn of the right cochlea. All 22 intracochlear electrodes were successfully inserted, and no complications, such as FNS and mis-insertion, occurred. We attribute this success to the use of modiolus-hugging electrodes. The results of postoperative speech perception were good and consistent with those of previous reports.

Conflict of interest

None.

References

[1] Nager GT. Ostenogenesis imperfecta of the temporal bone and its relation to otosclerosis. Ann Otol Rhinol Laryngol 1988;97:585–93.
[2] van der Hoeve J, de Kleyn A. Blaue sclerae, knochenbruechigkeit und schwerhoerighkeit. Albrecht Von Graefes Arch Klin Exp Ophthalmol 1918;95:81–93.
[3] Proscop DJ, Kuivaniemi H, Tromp G. Hereditable disorders of connective tissue. In: Isselbacher E, Braunwald JD, Wilson JB, Martin AS, Fauci DL, Kasper, editors. Harrison's principles of internal medicine. 13th ed., McGraw-Hill International; 1994. p. 2111–3.
[4] Pedersen U. Hearing loss in patients with osteogenesis imperfecta. A clinical and audiological study of 201 patients. Scand Audiol 1984;13:67–74.
[5] Streubel SO, Lustig LR. Cochlear implantation in patients with osteogenesis imperfecta. Otolaryngol Head Neck Surg 2005;132:735–40.
[6] Cohen BJ. Osteogenesis imperfecta and hearing loss. Ear Nose Throat J 1984;63:283–8.
[7] Rotteveel LJ, Beynon AJ, Mens LH, Snik AF, Mulder JJ, Mylanus EA. Cochlear implantation in 3 patients with osteogenesis imperfecta: imaging, surgery and programming issues. Audiol Neurootol 2009;13:73–85.
[8] Migirov L, Henkin Y, Hildesheimer M, Kronenberg J. Cochlear implantation in a child with osteogenesis imperfecta. Int J Pediatr Otorhinolaryngol 2003;67:677–80.
[9] Huang TS, Yen PT, Liu SY. Cochlear implantation in a patient with osteogenesis imperfecta and otospongiosis. Am J Otolaryngol 1998;19:209–12.
[10] Szilvássy J, Jóri J, Czigner J, Tóth F, Szilvássy Z, Kiss JG. Cochlear implantation in osteogenesis imperfecta. Acta Otorhinolaryngol Belg 1998;52:253–6.
[11] Mens LH, Mulder JJ. Averaged electrode voltages in users of the Clarion cochlear implant device. Ann Otol Rhinol Laryngol 2002;111:370–5.
[12] Sillence DO, Senn A, Danks DM. Genetic heterogeneity in osteogenesis imperfecta. J Med Genet 1979;16:101–16.
[13] Swinnen FK, De Leenheer EM, Goemaere S, Cremers CW, Coucke PJ, Dhooge IJ. Association between bone mineral density and hearing loss in osteogenesis imperfecta. Laryngoscope 2012;122:401–8.
[14] Kuurila K, Grenman R, Johansson R, Kaitila I. Hearing loss in children with osteogenesis imperfecta. Eur J Pediatr 2000;159:515–9.
[15] Tabor EK, Curtin HD, Hirsch BE, May M. Osteogenesis inperfecta tarda: appearance of the temporal bones at CT. Radiology 1990;175:181–3.
[16] Ruckenstein MJ, Rafter KO, Montes M, Bigelow DC. Management of far advanced otosclerosis in the era of cochlear implantation. Otol Neurotol 2001;22:471–4.
[17] Chen W, Meyer NC, McKenna MJ, Pfister M, McBride Jr DJ, Fukushima K, et al. Single-nucleotide polymorphisms in the COL1A1 regulatory regions are associated with otosclerosis. Clin Genet 2007;71:406–14.
[18] Bigelow DC, Kay DJ, Rafter KO, Montes M, Knox GW, Yousem DM. Facial nerve stimulation from cochlear implants. Am J Otol 1998;19:163–9.
[19] Cohen LT, Richardson LM, Saunders E, Cowan RS. Spatial spread of neural excitation on cochlear implant recipients: comparison of improved ECAP method and psychophysical forward masking. Hear Res 2003;179:72–87.
[20] Rotteveel LJ, Proops DW, Ramsden RT, Saeed SR, van Olphen AF, Mylanus EA. Cochlear implantation in 53 patients with otosclerosis: demographics, computed tomographic scanning, surgery, and complications. Otol Neurotol 2004;25:943–52.
[21] Roland Jr JT. A model for cochlear implant electrode insertion and force evaluation: results with a new electrode design and insertion technique. Laryngoscope 2005;115:1325–39.
[22] Kontorinis G, Lenarz T, Stöver T, Paasche G. Impact of the insertion speed of cochlear implant electrodes on the insertion forces. Otol Neurotol 2011;32:565–70.
[23] Berger G, Hawke M, Johnson A, Proops D. Histopathology of the temporal bone in osteogenesis imperfecta congenita: a report of 5 cases. Laryngoscope 1985;95:193–9.

Original Paper

Audiology & Neurotology

Audiol Neurotol 2013;18:335–343
DOI: 10.1159/000354620

Received: March 11, 2013
Accepted after revision: July 22, 2013
Published online: October 2, 2013

Evaluation of the Internal Structure of Normal and Pathological Guinea Pig Cochleae Using Optical Coherence Tomography

Akinobu Kakigi[a] Yuya Takubo[b] Naoya Egami[a] Akinori Kashio[a]
Munetaka Ushio[a] Takashi Sakamoto[a] Shinji Yamashita[b] Tatsuya Yamasoba[a]

[a]Department of Otolaryngology, Faculty of Medicine, and [b]Research Center for Advanced Science and Technology, The University of Tokyo, Tokyo, Japan

Key Words
Cochlea · Optical coherence tomography · Endolymphatic hydrops · Strial atrophy · Organ of Corti

Abstract
Optical coherence tomography (OCT) makes it possible to visualize the internal structures of several organs, such as the eye, in vivo. Although visualization of the internal structures of the inner ear has been used to try and identify certain pathological conditions, attempts have failed mainly due to the thick bony capsule surrounding this end organ. After decalcifying the bony wall of the cochlea with ethylenediamine tetraacetic acid, we could clearly visualize its internal structures by using OCT. We identified endolymphatic hydrops, strial atrophy and damage to the organ of Corti, evident as a distention of Reissner's membrane, thinning of the lateral wall and flattening of the organ of Corti, respectively. When specimens embedded in paraffin, sliced and stained with hematoxylin and eosin (HE) were examined under a light microscope, the OCT images of normal and pathological cochleae were virtually identical with those of the HE specimens, except that the HE specimens exhibited several artifacts unrecognized in OCT images, which were considered to be induced during the preparation process. Since OCT enables one to obtain arbitrary plane images by manipulating the slice axis of the specimens and avoids any misinterpretation due to artifacts induced during histological preparation, our technique would be useful for examining cochlear pathologies without or prior to histological evaluations.

Introduction

Structural integrity of the cochlea is required to maintain normal auditory function. Certain types of cochlear pathologies have been known to be closely associated with impaired auditory function. Since the cochlea is housed deeply within the temporal bone, however, it is extremely difficult to examine its structure in vivo. Structural observation has primarily been limited to histological methods, which require several procedures such as chemical fixation, dissection of the tissues, embedment in a mold such as paraffin, and sectioning. These procedures can introduce significant changes in tissue integrity and organization [Slepecky and Ulfendahl, 1988; Brunschwig and Salt, 1997], limiting the generality and overall value of results. To better visualize the internal structure of the cochlea, an emerging noninvasive imaging modality, optical coherence tomography (OCT), has been applied.

KARGER

1420–3030/13/0185–0335$38.00/0

E-Mail karger@karger.com
www.karger.com/aud

Akinobu Kakigi
Department of Otolaryngology, Faculty of Medicine, University of Tokyo
7-3-1 Hongo, Bunkyo-ku
Tokyo 113-8655 (Japan)
E-Mail kakigi-tky@umin.ac.jp

OCT uses low-coherence interferometry to produce a two-dimensional image of internal tissue microstructures [Huang et al., 1991]. It uses light to discern intrinsic differences in tissue structure and uses coherence gating to localize the origin of the reflected optic signal. Internal tissue microstructures can be visualized with axial and lateral spatial resolutions in the order of 10 μm and a depth of penetration of approximately 2–3 mm depending on tissue translucency. This technology has become widely established for clinical applications in the fields of ophthalmology and dermatology to visualize the translucent tissues of the eye [Izatt et al., 1994] and superficial tissues of the skin [Welzel, 2001].

Clinical use of OCT has since been extended to the fields of cardiology and gastroenterology in visualizing deeper structures such as coronary vessels [Jang et al., 2002] and the gastrointestinal tract [Shen and Zuccaro, 2004]. Most recently, OCT has been used in the field of otolaryngology to visualize the larynx [Wong et al., 2005]. However, clinical use of OCT has been limited in other organs including the inner ear because of its relatively limited depth of penetration and the turbidity of most biological tissues. In fact, previous studies allowed visualization of only limited areas of the cochleae [Wong et al., 2004; Lin et al., 2008; Sepehr et al., 2008; Subhash et al., 2010]. For example, Sepehr et al. [2008] drilled the otic capsule of pigs obtained within 1 h of sacrifice and found that in the areas of thinned bone, acceptable images were obtained of the spiral ligament, stria vascularis, Reissner's membrane, basilar membrane, tectorial membrane, scala media, scala tympani and scala vestibuli; however, the bone was too thick for adequate light penetration in the areas where it was not thinned.

Subhash et al. [2010] obtained in vivo OCT images of a portion of the apical, middle and basal turns of the mouse cochlea through a surgically prepared opening via the bone of the bulla. They demonstrated that spectral-domain OCT could be used for in vivo imaging of important morphological features within the mouse cochlea, such as the otic capsule and structures within, including Reissner's membrane, the basilar membrane, the tectorial membrane, the organ of Corti and the modiolus of the apical and middle turns, but the resolution and quality were unsatisfactory.

In the current study, we observed the cochleae by OCT after decalcification of the otic bony capsule. We could clearly visualize normal internal structures of the cochleae and identify endolymphatic hydrops (EH), strial atrophy and damage to the organ of Corti, which appeared as a distention of Reissner's membrane, thinning of the lateral wall and flattening of the organ of Corti, respectively. This technology can prevent the misinterpretation of histological findings due to artifacts induced during histological preparation and thus is of great value in investigating the internal structural change of various types of cochlear damage.

Materials and Methods

Animals

A total of 20 Hartley guinea pigs with a positive Preyer reflex and weighing approximately 300 g were used. They were allocated to the following four groups, each consisting of 5 animals: (1) normal control group (no surgical procedure or treatment); (2) EH group (electrocauterization of the endolymphatic sac (ES), and a 4-week feeding); (3) kanamycin sulfate-ethacrynic acid (KM-EA) group (no surgical procedures, but intravenous administration of KM and EA and a 2-day feeding); and (4) streptomycin sulfate (SM) group (perilymphatic perfusion with 20% SM and a 4-month feeding). These experiments were approved by the Tokyo University animal care and use committee, and conformed to the Animal Welfare Act and the guiding principles for animal care produced by the Ministry of Education, Culture, Sports and Technology, Japan.

Surgical Procedure for the Electrocauterization of ES

EH can be either primary or secondary. Primary idiopathic EH (known as Ménière's disease) occurs for no known reason, while secondary EH appears to occur in response to an event or underlying condition (e.g. following head trauma or ear surgery, or with other inner ear disorders, allergies or systemic disorders such autoimmune disorders). EH was initially reported in patients with Ménière's disease independently by Yamakawa [1938] and Hallpike and Cairns [1938] and has since been found to be frequent in patients with Ménière's disease. EH represents a histopathological finding in which the structures bounding the endolymphatic space are distended by an enlargement of endolymphatic volume. The most widely studied animal model of EH was created by surgical ablation of the endolymphatic duct and sac in guinea pigs [Kimura and Schuknecht, 1965; Kimura, 1967].

To induce EH, we performed electrocauterization of the ES. Animals were anesthetized with an intraperitoneal injection of ketamine (35 mg/kg) and xylazine (5 mg/kg) and received local anesthesia with Xylocaine in sterile conditions. Then, they were placed in a prone position with a head holder and underwent a dorsal midline scalp incision under a Carl Zeiss operation microscope. The left occipital bone was removed to visually expose the ES via an epidural occipital approach. Then, the extraosseous portion of the sac was cauterized electrically so as not to injure the sigmoid sinus with the bipolar electrocoagulator (Surgitron Model FFPF; Ellman International Inc., Hewlett, N.Y., USA). The skin incision was sutured and the animals were allowed to survive for 4 weeks.

Procedures for Intravenous Administration of KM and EA

Auditory hair cells can be damaged and lost as a consequence of acoustic trauma, treatment with ototoxic agents, infections, autoimmune pathologies and genetic susceptibilities or as a part of the aging process. The loss of auditory hair cells in the human cochlea is a leading cause of permanent hearing deficits, currently affecting an estimated 600 million worldwide. In recent studies, loop diuret-

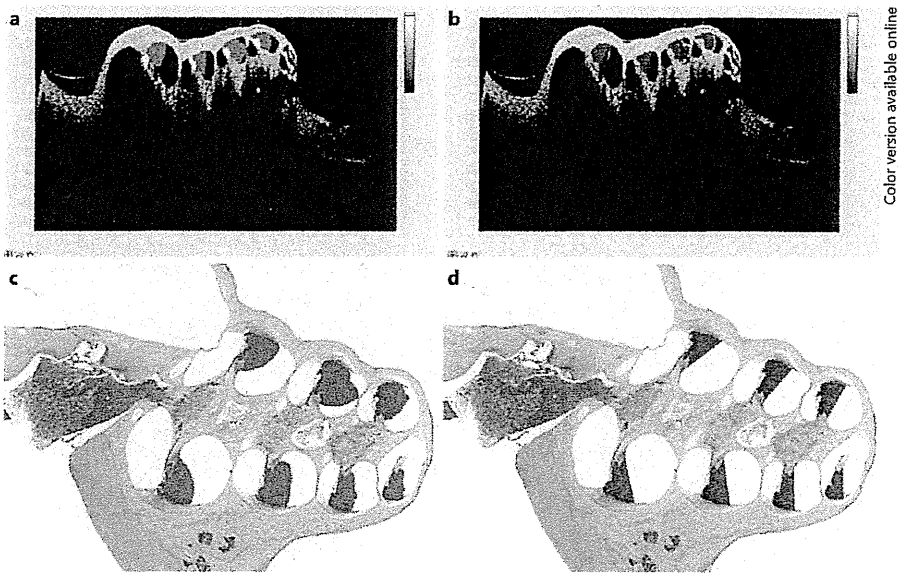

Fig. 1. Parameters for quantitative assessment of changes in endolymphatic space, organ of Corti and lateral wall. **a** Cross-sectional area of the dilated scala media (red areas), organ of Corti (yellow areas) and upper part of the lateral wall over the extended line of the lower level of the basilar membrane (green area) in an OCT image. **b** Cross-sectional area of the original scala media (blue areas) enclosed by a straight line segment. This line segment represents the position of the idealized Reissner's membrane at the upper margin of the stria vascularis to its normal medial attachment at the spiral limbus. **c** Cross-sectional area of the dilated scala media (red areas) of an HE specimen. **d** Cross-sectional area of the original scala media (blue areas) of an HE specimen. Colors refer to the online version only.

ics have been used to augment the ototoxic effect of aminoglycoside antibiotics and eliminate hair cells in mammals [Xu et al., 1993; Yamasoba and Kondo, 2006; Kashio et al., 2007; Taylor et al., 2008].

To induce degeneration of the organ of Corti, animals were given KM (Meiji, Tokyo, Japan) and EA (Sigma-Aldrich). They were anesthetized with an intraperitoneal injection of ketamine (35 mg/kg) and xylazine (5 mg/kg). A single dose of KM (400 mg/kg) was injected subcutaneously; 2 h after the KM injection, EA (50 mg/kg) was infused into the jugular vein as previously described [Yamasoba and Kondo, 2006]. The animals were then allowed to survive for 2 days after deafening.

Procedures for Perilymphatic Perfusion with 20% SM

Strial atrophy is one of the leading causes of deafness and three major etiologic factors have been reported: hereditary strial hypoplasia/atrophy [Gates et al., 1999; Ohlemiller et al., 2006], aging [Schuknecht and Gacek, 1993] and ototoxicity due to loop diuretics or the erythromycin group of antibiotics [Arnold et al., 1981; McGhan and Merchant, 2003].

To induce both hair cell loss and strial atrophy, animals underwent perilymphatic perfusion with 20% SM (Meiji) dissolved in Ringer's solution (Fuso, Osaka, Japan). The animals were anesthetized with an intraperitoneal injection of ketamine (35 mg/kg) and xylazine (5 mg/kg). The left cochlea was exposed using the lateral approach, and both the scala tympani and the scala vestibuli of four cochlear turns were perfused as follows. A 20% SM solution was gently perfused into the scala tympani through the round window membrane until the solution flowed out from the drilled hole adjacent to the oval window, as previously described [Terayama et al., 1977]. After the perfusion, the tympanic cavity was cleaned, the skin incision closed and the animals allowed to survive for 4 weeks.

OCT and Histological Observations

To observe the cochleae by OCT, all animals were given physiological saline from the left ventricle under deep anesthesia with ketamine and xylazine and fixed with 10% formalin. Both temporal bones were obtained immediately following the fixation and kept in a 10% formalin solution for 1 week. Subsequently, the specimens underwent decalcification in ethylenediamine tetraacetic acid (EDTA) for 14 days. Then we obtained midmodiolar images of the cochleae by using the Santec OCT system controlled by Inner Vision (Santec Co., Aichi, Japan). The characteristics of the Santec OCT system were as follows. The center wavelength band was 1,320 nm and the band width 90 nm. The axial and lateral resolutions were 12.0 and 17.0 μm, respectively. The measurement speed and frame rate were 50,000 lines/scan and 100 frames/s, respectively. The image depth and width were 6.0 and 10.0 mm, respectively. After OCT images were obtained, the temporal bones were dehydrated in increasingly higher concentrations of alcohol, embedded in paraffin and cut serially at 6 μm in the plane parallel to the modiolus to obtain approximately the same plane as the OCT image. The sections were stained with hematoxylin and eosin (HE) and observed under a light microscope [light microscopic mode of the BZ-9000 fluorescence microscope (Keyence, Osaka, Japan) controlled by BZ-II Analyzer (Keyence) software].

Quantitative Assessment of Endolymphatic Space, Organ of Corti and Lateral Wall

We used the digital image measurement software Micro Analyzer version 1.1 (Nippon Poladigital Co. Ltd, Tokyo, Japan) for quantitative assessment. In the EH group, we compared the degree of EH between OCT and HE images. For the quantitative assessment of endolymphatic space variations of the cochlea, we measured the increase in the cross-sectional area of the scala media (IR-S) over that in the midmodiolar sections. For this analysis, we used the following two parameters in the basal, second, third and apical turns, not including the hook portion: (1) the cross-sectional area of the dilated scala media (fig. 1a, c; red areas) and (2) the cross-sectional area of the original scala media (fig. 1b, d; blue areas) which were enclosed by a straight line segment. This line segment represents the position of the idealized Reissner's membrane at the upper margin

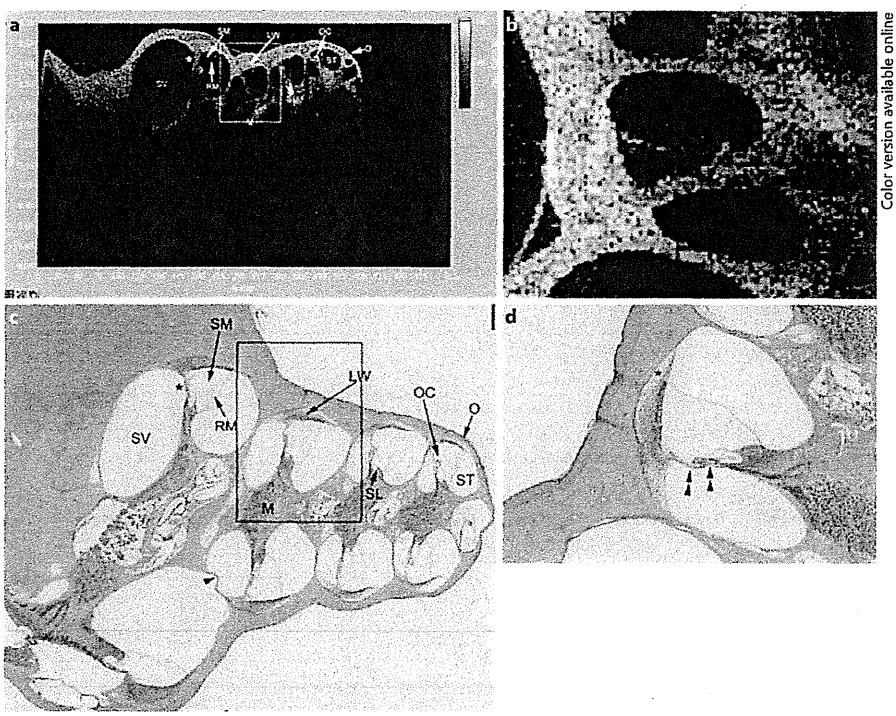

Color version available online

Fig. 2. a Representative cross-sectional OCT image of all turns of the spiral-shaped cochlea. **b** Magnified image (turned 90°) of the rectangular area in **a**. **c** Cross-sectional image of an HE specimen, using a light microscope. HE specimens exhibited several artifacts such as bending of the interscalar septum and basilar membrane and folding of Reissner's membrane as a consequence of separating the spiral ligament from the bony wall. The proportion of the area of the organ of Corti is smaller in the HE specimen (star) than in the OCT image (**a**; white star), especially in the basal turn. **d** Magnified image of the rectangular area in **c**. O = Otic capsule; M = modiolus; RM = Reissner's membrane; OC = organ of Corti; SL = spiral limbus; LW = lateral wall consisting of stria vascularis and spiral ligament; ST = scala tympani; SM = scala media; SV = scala vestibuli; arrowhead = bending of interscalar septum; double arrowheads = bending of basilar membrane; white arrowheads = folding of Reissner's membrane; asterisk = separating spiral ligament from bony wall.

of the stria vascularis to its normal medial attachment at the spiral limbus. From these parameters, we calculated the increase (%) in IR-S in the four turns with the following formula:

Total IR-S (%) = 100 × (red area – blue area)/blue area

Statistical Analysis

Data are presented as means ± SD, and they were compared by the paired Student t test. Differences were regarded as significant when $p < 0.05$.

We compared the degree of flattening of the organ of Corti and strial atrophy between the normal control and KM-EA groups and between the normal control and SM groups, respectively. To analyze the flattening of the organ of Corti, we used the following parameter in the basal, second, third and apical turns, not including the hook portion: the cross-sectional area of the organ of Corti (fig. 1a; yellow areas). Data for each turn were separately compared by Student's t test, and a difference was regarded as significant when $p < 0.05$. For the analysis of strial atrophy, we used the following parameter in the second turn: the cross-sectional area of the upper part of the lateral wall over the extended line of the lower level of the basilar membrane (fig. 1a; green area). We selected the second turn for the assessment because there was no proliferative change such as fibrosis.

Results

Normal Control Group

OCT provided detailed internal structures of the normal cochleae. We clearly identified not only the otic capsule and the modiolus, but also Reissner's membrane, the organ of Corti, the spiral limbus, the lateral wall consisting of the stria vascularis and spiral ligament in all four turns of the midmodiolar section (fig. 2a, b). The scalae tympani, media and vestibuli were clearly distinguishable. The OCT images were virtually identical with the corresponding histological sections (fig. 2c, d), although the HE specimens exhibited several artifacts such as the bending of the interscalar septum and basilar membrane and the folding of Reissner's membrane as a consequence of the separation of the spiral ligament from the bony wall. Concerning the organ of Corti, the proportion of the area was smaller in the HE specimen than in the OCT image, especially in the basal turn.

EH Group

OCT clearly demonstrated the presence of EH in all 5 cases 4 weeks after electrocauterization of the ES. In a case shown in figure 3a, mild but distinct hydrops was observed in the basal and second turns, and the hydrops was most evident in the third turn (fig. 3b, d). The spiral ligament, stria vascularis and organ of Corti appeared normal. A midmodiolar HE-stained section in this ear showed similar histological findings (fig. 3c), although the extent of EH was greater in the histological specimens

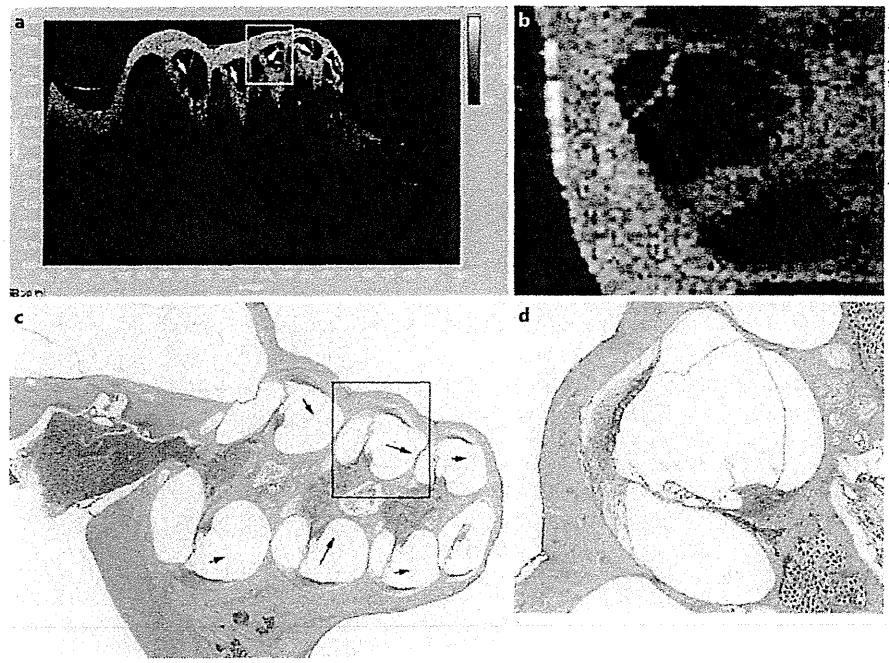

Fig. 3. **a** Representative cross-sectional OCT image of the cochlea in animals with electrocauterization of the ES. Mild but distinct hydrops was found in the basal and second turns, and hydrops was most evident in the third turn. **b** Magnified image of the rectangular area in **a**. **c** Cross-sectional image of an HE specimen, using a light microscope. A midmodiolar HE-stained section in this ear showed similar histological findings, although the extent of EH was greater in the histological specimens than in the OCT images. There are several artifacts similar to those seen in the normal cochlea. Note that hydrops was most evident in this turn. **d** Magnified image of the rectangular area in **c**. Arrows = Distention of Reissner's membrane.

than in the OCT images (fig. 4). Further, there were several artifacts similar to those seen in the normal cochlea. Figure 4 shows the IR-S in OCT and HE images: 54.3 ± 4.05% and 62.4 ± 6.51%, respectively. The IR-S was statistically larger in the HE than in the OCT images (paired Student's t test, $p < 0.05$).

KM-EA Group

Two days after the treatment with KM and EA, all animals lost the Preyer reflex and exhibited degeneration of the organ of Corti in all turns (fig. 5a). In a case shown in figure 5b, the flattening of the organ of Corti was obvious in the third and apical turns, whereas the spiral ligament and stria vascularis appeared normal. A slight collapse of Reissner's membrane was seen in all four turns. A midmodiolar HE-stained section in this ear showed similar histological findings, except that there was no collapse of Reissner's membrane (fig. 5e, f). The difference regarding Reissner's membrane between the OCT and histological findings may have been caused by histological preparation. Further, there were several artifacts similar to those seen in the normal cochlea. To assess the effects of KM-EA treatment on the organ of Corti, a comparison of the normalized size ratio of the organ of Corti (size of the targeted organ of Corti/average of the size of the normal organ of Corti) was made between the normal control and KM-EK groups, using OCT images. The normalized size

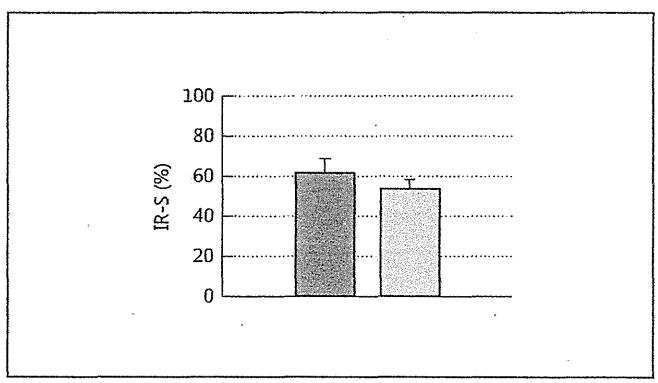

Fig. 4. Comparison of IR-S between OCT (light gray) and HE (dark gray) images. The IR-S (means ± SD) on the OCT and HE images were 54.3 ± 4.05% (n = 5) and 62.4 ± 6.51% (n = 5), respectively. The IR-S on the HE images was statistically larger than that on the OCT images (paired Student's t test, $p < 0.05$).

ratios of the basal, second, third and apical turns were 0.63 ± 0.14, 0.78 ± 0.16, 0.51 ± 0.10 and 0.58 ± 0.14, respectively, in the KM-EA group (n = 5; fig. 6). The KM-EA treatment resulted in a marked decrease in normalized size ratio of the organ of Corti. The decreases in the basal, second, third and apical turns were significant at $p < 0.001$, $p < 0.05$, $p < 0.001$ and $p < 0.05$, respectively (Student's t test).

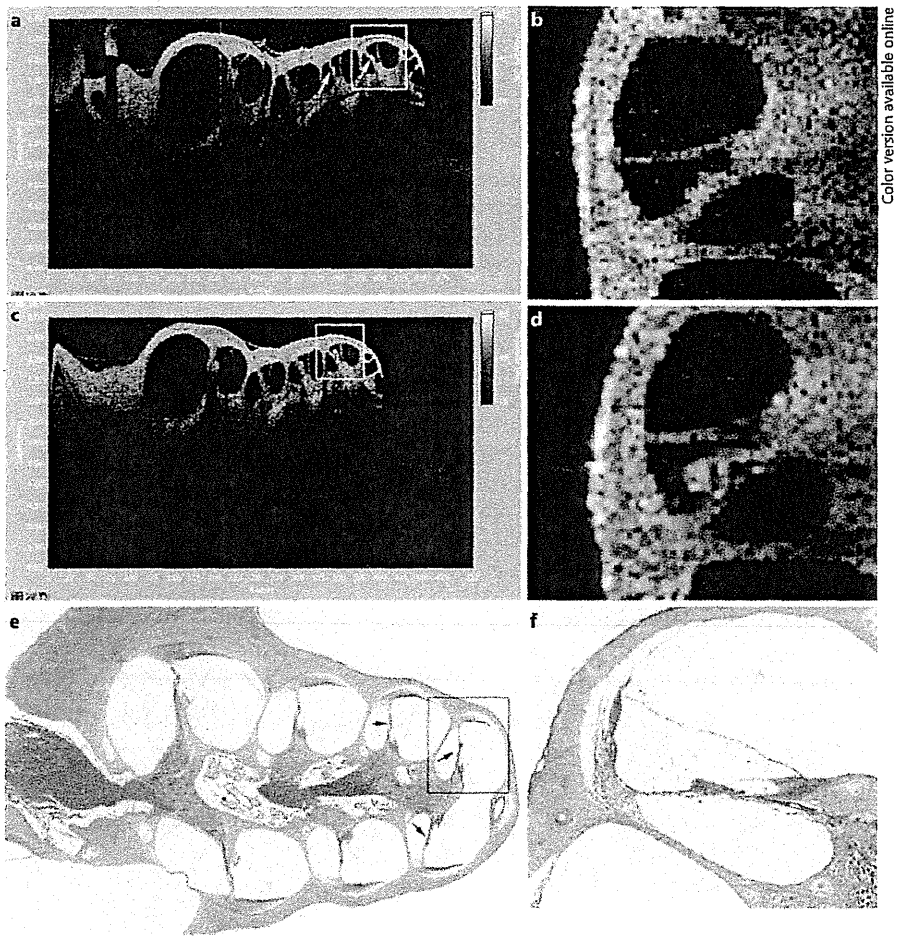

Fig. 5. **a** Representative cross-sectional OCT image of the cochlea in animals with intravenous administration of KM and EA. The flattening of the organ of Corti was obvious in the third and apical turns. The spiral ligament and stria vascularis appeared normal. A slight collapse of Reissner's membrane was seen in all four turns. **b** Magnified image of the rectangular area in **a**. **c** Representative cross-sectional OCT image of the cochlea in the normal group. **d** Magnified image of the rectangular area in **c**. **e** A midmodiolar HE-stained section showed similar histological findings, although there was no collapse of Reissner's membrane. There are several artifacts similar to those seen in the normal cochlea. Note that flattening of the organ of Corti was evident. **f** Magnified image of the rectangular area in **e**. Arrows = Flattening of the organ of Corti.

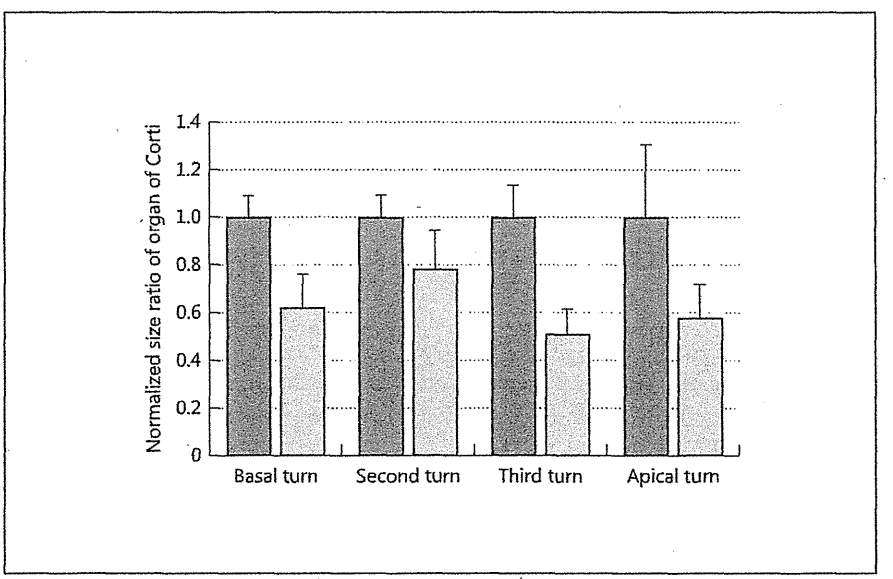

Fig. 6. Comparison of normalized size ratio (size of organ of Corti/averaged size of normal organ of Corti) of organ of Corti between normal control (dark gray) and KM-EA (light gray) groups, using OCT images. The normalized size ratios (means ± SD) of the basal, second, third and apical turns were 1.00 ± 0.09, 1.00 ± 0.09, 1.00 ± 0.14 and 1.00 ± 0.31, respectively, in the normal control group (n = 5), and 0.63 ± 0.14, 0.78 ± 0.16, 0.51 ± 0.10 and 0.58 ± 0.14, respectively, in the KM-EA group (n = 5). The decreases in the basal, second, third and apical turns were significant at $p < 0.001$, $p < 0.05$, $p < 0.001$ and $p < 0.05$, respectively (Student's t test).

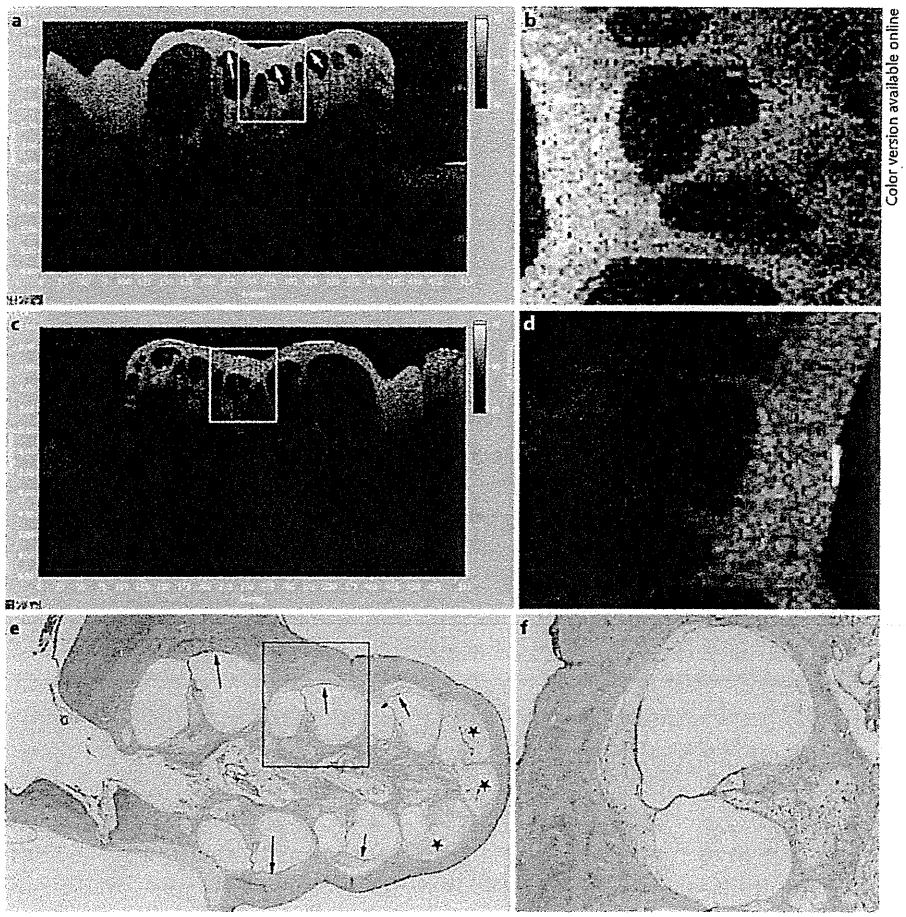

Color version available online

Fig. 7. **a** Representative cross-sectional OCT image of the cochlea in animals with perilymphatic perfusion with SM. Strial atrophy and flattening of the organ of Corti were seen in the basal, second and third turns. The strial atrophy reflected that the curvature of the medial surface increased in the lateral wall. A remarkable collapse of Reissner's membrane was also seen. In the apical turn, the fibrosis of the organ was remarkable. **b** Magnified image of the rectangular area in **a**. **c** Representative cross-sectional OCT image of the cochlea in the control ear. **d** Magnified image of the rectangular area in **c**. **e** Optical cross-sectional image of an HE specimen, using a light microscope. There are the same artifacts in the HE specimen as seen in the normal cochlea. **f** Magnified image of the rectangular area in **e**. Arrows = Strial atrophy; stars = fibrosis.

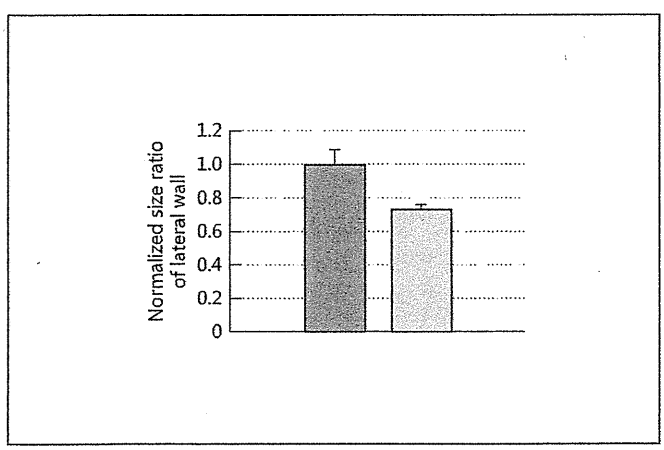

Fig. 8. Comparison of normalized size ratio (size of lateral wall/averaged size of normal lateral wall) of lateral wall between normal control (dark gray) and SM (light gray) groups, using OCT images. The normalized size ratio (mean ± SD) of the second turn was 1.00 ± 0.08 in the normal control group (n = 5) and 0.74 ± 0.02 in the SM group (n = 5). The decrease in the second turn was significant at $p < 0.001$ (Student's t test).

SM Group

The strial atrophy and damage to the organ of Corti were evident in all cases 4 weeks after perilymphatic perfusion with 20% SM (fig. 7a, b). Strial atrophy and flattening of the organ of Corti were seen mostly in the basal, second and third turns. The strial atrophy reflected that the curvature of the medial surface increased in the lateral wall. The remarkable collapse of Reissner's membrane was also seen mostly in the basal, second and third turns. In some animals, fibrosis was observed in the apical part of the cochlea. The OCT images were comparable with the corresponding histological sections (fig. 7e, f), although the loss of spiral ganglion cells observed in the HE specimen could not be visualized by OCT because of the limited spatial resolution and depth of penetration. To assess the effects of SM treatment on the lateral wall, a comparison of the normalized size ratio of the lateral wall was made between the normal control and SM groups, using OCT images. The normalized size ratio of the second turn was 0.74 ± 0.02 in the SM group (n = 5;

fig. 8). SM treatment resulted in a marked decrease in the normalized size ratio of the lateral wall. The decrease in the second turn was significant at $p < 0.001$ (Student's t test).

Discussion

The current study demonstrated that by decalcifying the bony wall of the cochlea with EDTA, the internal structures of the cochlea could be clearly visualized by OCT. The OCT images of the normal cochleae were significantly improved compared with those from previous reports [Wong et al., 2004; Lin et al., 2008; Sepehr et al., 2008; Subhash et al., 2010]. We found that OCT could prevent unnecessary misinterpretations due to artifacts introduced during the preparation of specimens for conventional histological examination. We could also demonstrate that three major cochlear pathologies, i.e. EH, hair cell degeneration and strial atrophy, could be clearly visualized by using OCT.

EH is commonly observed in patients with Ménière's disease and may also occur following head trauma or ear surgery, or in other inner ear disorders, allergies or systemic disorders such autoimmune disorders. The pathophysiology of Ménière's disease has been studied using animal models, and surgical ablation of the endolymphatic duct and sac of guinea pigs [Kimura and Schuknecht, 1965; Kimura, 1967] has most widely been used. It is impossible to determine the presence of EH by using physiological tests such as the auditory brainstem response or caloric test, since such examinations provide only information on the extent of damage to hearing or vestibular function. Thus, it is mandatory to evaluate the presence/absence and extent of EH by histological examination in animals. Schuknecht [1987, 1993] established a standard procedure for the morphological study of the human temporal bone that involved formalin fixation, EDTA decalcification, celloidin embedding and serial sectioning. Celloidin and paraffin are the two common embedding media used for histopathologic study of the human temporal bone by light microscopy. Although celloidin embedding permits excellent morphologic assessment, celloidin is difficult to remove, and there are significant restrictions on success with immunostaining. Other potential disadvantages of the use of celloidin include the length of time needed for embedment. Embedding in paraffin allows immunostaining to be performed, but the preservation of cellular detail within the membranous labyrinth is relatively poor [Merchant et al., 2006]. During the preparation process, the specimen must be embedded in a mold such as paraffin or celloidin, and such a process, especially with paraffin, is known to induce significant artifacts, making it difficult to evaluate the extent of EH. Compared with the OCT images in our study, paraffin-embedded HE specimens exhibited EH to a greater extent and also showed artifacts such as bending of the interscalar septum and basilar membrane and folding of Reissner's membrane. These findings suggest that estimating the extent of EH and associated tissue damage can be done more precisely using OCT images than by histological evaluation, especially using paraffin-embedded HE specimens. Further, the specimen can be easily used for molecular and immunohistochemical techniques after OCT imaging.

We also observed that OCT could visualize the degeneration of the organ of Corti, collapse of Reissner's membrane and strial atrophy 2 days after systemic administration of a combination of KM and EA and 4 weeks after perfusion with 20% SM throughout the cochlea. An intravenous administration of KM and EA induces hair cell degeneration and scar formation, which start 3 h after drug administration [Raphael and Altschuler, 1991]. In Raphael and Altschuler's report, mild flattening of the organ of Corti was seen from 9 h after drug administration. At this time, the outer hair cells from all three rows are replaced by supporting cells, which fill the entire space between the tunnel of Corti and Hensen cells. However, the inner hair cells are present and the shape of the organ of Corti is preserved. In our study, OCT could detect such degeneration as a reduction in the size of the organ of Corti, which could not be observed in the basal turn of an HE-stained section because of the artifacts produced (fig. 2a, b). Further, OCT could detect a mild collapse of Reissner's membrane, which again could not be detected in HE-stained sections. These findings suggest that estimating the extent of the degeneration of the organ of Corti and associated tissue damage (e.g. collapse of Reissner's membrane) can be done more precisely by using OCT images than histological evaluation, especially with paraffin-embedded HE specimens. Conversely, although OCT could detect severe degeneration of the organ of Corti, strial atrophy and remarkable collapse of Reissner's membrane in the SM group, it could not detect the loss of spiral ganglion cells, which could be observed in the HE specimens.

The method shown here cannot be applied to clinical evaluations of pathology in the cochlea. Therefore, we still need other novel technologies to improve the transparency and translucency of OCT.

Conclusions

By decalcifying the bony wall of the cochlea, we could clearly and widely visualize the internal structures of normal and pathological cochleae. We could easily manipulate the slice axis to obtain arbitrary plane views using OCT, and we could demonstrate EH, strial atrophy and damage to the organ of Corti as a distention of Reissner's membrane, a thinning of the lateral wall and a flattening of the organ of Corti, respectively. The OCT images of normal and pathological cochleae were virtually identical with those of HE specimens, except that the extent of EH was overestimated in histological images compared with OCT images and that there were several artifacts in the HE specimen, such as bending of the interscalar septum and basilar membrane, folding of Reissner's membrane, separation of the spiral ligament from the bony wall, and flattening of the organ of Corti in the basal turn, which were not seen in the OCT images. These findings indicate that observing the decalcified cochlea by using OCT would be of great value when examining cochlear pathology, especially EH, prior to or without histological examinations.

Disclosure Statement

This study was supported by a Health and Labor Science Research Grant for Research on Specific Diseases (Vestibular Disorders) from the Ministry of Health, Labor and Welfare of Japan, and by grants from the Ministry of Education, Science, Culture and Sports, Japan (No. 21592159) and by the Funding Program for Next Generation World-Leading Researchers (NEXT Program) of the Japan Society for the Promotion of Science (JSPS). We have no conflicts of financial interest in this paper.

References

Arnold W, Nadol JB Jr, Weidauer H: Ultrastructural histopathology in a case of human ototoxicity due to loop diuretics. Acta Otolaryngol 1981;91:399–414.

Brunschwig AS, Salt AN: Fixation-induced shrinkage of Reissner's membrane and its potential influence on the assessment of endolymph volume. Hear Res 1997;114:62–68.

Gates GA, Couropmitree NN, Myers RH: Genetic associations in age-related hearing thresholds. Arch Otolaryngol Head Neck Surg 1999; 125:654–659.

Hallpike CS, Cairns HWB: Observations of the pathology of Ménière's syndrome. Proc R Soc Med 1938;31:1317–1336.

Huang D, Swanson EA, Lin CP, Schuman JS, Stinson WG, Chang W, Hee MR, Flotte T, Gregory K, Puliafito CA, Fujimoto JG: Optical coherence tomography. Science 1991;254:1178–1181.

Izatt JA, Hee MR, Swanson EA, Lin CP, Huang D, Schuman JS, Puliafito CA, Fujimoto JG: Micrometer-scale resolution imaging of the anterior eye in vivo with optical coherence tomography. Arch Ophthalmol 1994;112:1584–1589.

Jang IK, Bouma BE, Kang DH, Park SJ, Park SW, Seung KB, Cho, KB, Shishkov M, Schlendorf K, Pomerantsev E, Houser SL, Aretz HT, Tearney GJ: Visualization of coronary atherosclerotic plaques in patients using optical coherence tomography: comparison with intravascular ultrasound. J Am Coll Cardiol 2002;39:604–609.

Kashio A, Sakamoto T, Suzukawa K, Asoh S, Ohta S, Yamasoba T: A protein derived from the fusion of TAT peptide and FNK, a Bcl-x_L derivative, prevents cochlear hair cell death from aminoglycoside ototoxicity in vivo. J Neurosci Res 2007;85:1403–1412.

Kimura RS: Experimental blockage of the endolymphatic duct and sac and its effect on the inner ear of the guinea pig. Ann Otol Rhinol Laryngol 1967;76:664–687.

Kimura RS, Schuknecht HF: Membranous hydrops in the inner ear of the guinea pig after obliteration of the endolymphatic sac. Pract Otorhinolaryngol (Basel) 1965;27:343–354.

Lin J, Staecker H, Jafri MS: Optical coherence tomography imaging of the inner ear: a feasibility study with implications for cochlear implantation. Ann Otol Rhinol Laryngol 2008; 117:341–346.

McGhan LJ, Merchant SN: Erythromycin ototoxicity. Otol Neurotol 2003;24:701–702.

Merchant SN, Burgess B, O'Malley J, Jones D, Adams JC: Polyester wax: a new embedding medium for the histopathologic study of human temporal bones. Laryngoscope 2006;116: 245–249.

Ohlemiller KK, Lett JM, Gagnon PM: Cellular correlates of age-related endocochlear potential reduction in a mouse model. Hear Res 2006;220:10–26.

Raphael Y, Altschuler RA: Scar formation after drug-induced cochlear insult. Hear Res 1991; 51:173–184.

Schuknecht H: Temporal bone collections in Europe and the United States: observations on a productive laboratory, pathologic findings of clinical relevance, and recommendations. Ann Otol Rhinol Laryngol 1987;130:1–19.

Schuknecht H: Methods of removal, preparation and study; in Schuknecht H (ed): Pathology of the Ear, ed 2. Philadelphia, Lea & Febiger, 1993, pp 1–29.

Schuknecht HF, Gacek MR: Cochlear pathology in presbycusis. Ann Otol Rhinol Laryngol 1993;102:1–16.

Sepehr A, Djalilian HR, Chang JE, Chen Z, Wong BJ: Optical coherence tomography of the cochlea in the porcine model. Laryngoscope 2008;118:1449–1451.

Shen B, Zuccaro G Jr: Optical coherence tomography in the gastrointestinal tract. Gastrointest Endosc Clin N Am 2004;14:555–571, x.

Slepecky N, Ulfendahl M: Glutaraldehyde induces cell shape changes in isolated outer hair cells from the inner ear. J Submicrosc Cytol Pathol 1988;20:37–45.

Subhash HM, Davila V, Sun H, Nguyen-Huynh AT, Nuttall AL, Wang RK: Volumetric in vivo imaging of intracochlear microstructures in mice by high-speed spectral domain optical coherence tomography. J Biomed Opt 2010; 15:036024.

Taylor RR, Nevill G, Forge A: Rapid hair cell loss: a mouse model for cochlear lesions. J Assoc Res Otolaryngol 2008;9:44–64.

Terayama Y, Kaneko Y, Kawamoto K, Sakai N: Ultrastructural changes of the nerve elements following disruption of the organ of Corti. I. Nerve elements in the organ of Corti. Acta Otolaryngol 1977;83:291–302.

Welzel J: Optical coherence tomography in dermatology. Skin Res Technol 2001;7:1–9.

Wong BJ, Jackson RP, Guo S, Ridgway JM, Mahmood U, Su J, Shibuya TY, Crumley RL, Gu M, Armstrong WB, Chen Z: In vivo optical coherence tomography of the human larynx: normative and benign pathology in 82 patients. Laryngoscope 2005;115:1904–1911.

Wong BJ, Zhao Y, Yamaguchi M, Nassif N, Chen Z, de Boer JF: Imaging the internal structure of the rat cochlea using optical coherence tomography at 0.827 μm and 1.3 μm. Otolaryngol Head Neck Surg 2004;130:334–338.

Xu SA, Shepherd RK, Chen Y, Clark GM: Profound hearing loss in the cat following the single co-administration of kanamycin and ethacrynic acid. Hear Res 1993;70:205–215.

Yamakawa K: Über die pathologische Veränderung bei einem Ménière-Kranken. J Otolaryngol Soc Jpn 1938;4:2310–2312.

Yamasoba T, Kondo K: Supporting cell proliferation after hair cell injury in mature guinea pig cochlea in vivo. Cell Tissue Res 2006;325:23–31.

Acta Oto-Laryngologica. 2013; 133: 1128–1132

informa
healthcare

ORIGINAL ARTICLE

Effects of EAS cochlear implantation surgery on vestibular function

KEITA TSUKADA[1], HIDEAKI MOTEKI[1,2], HISAKUNI FUKUOKA[1], SATOSHI IWASAKI[2] & SHIN-ICHI USAMI[1]

[1]*Department of Otolaryngology and* [2]*Department of Hearing Implant Science, Shinshu University School of Medicine, Matsumoto City, Japan*

Abstract

Conclusions: The patients who received electric acoustic stimulation (EAS) cochlear implantation had relatively good vestibular function compared with the patients who did not have residual hearing. The vestibular function was well preserved after atraumatic EAS surgery. The round window approach and soft electrode are preferred to decrease the risk of impairing vestibular function. *Objectives:* The aim of this study was to examine the characteristic features of vestibular functions before and after implantations in patients undergoing EAS. *Methods:* Vestibular functions in patients who underwent EAS implantation were examined by caloric testing and vestibular evoked myogenic potential (VEMP) in 11 patients before and in 13 patients after implantation. *Results:* Preoperative evaluation showed that of the 11 patients, most (73%) had good vestibular function. One of 11 patients (9%) had decreased response in postoperative VEMP but all of the patients had unchanged results in postoperative caloric testing.

Keywords: *Cochlear implant, VEMP, caloric test, preservation*

Introduction

Recently, a series of reports have shown the efficiency of electric acoustic stimulation (EAS) in patients with residual acoustic hearing in the lower frequencies [1]. The development of techniques such as soft surgery when performing cochleostomy [2], round window insertion [3], use of atraumatic electrodes [4,5], and postoperative steroid administration has enabled preservation of residual hearing after cochlear implantation (CI) surgery.

Current techniques of CI also facilitate remarkable improvement in hearing ability. However, consideration must still be given to the complications that can accompany a CI.

One possible such complication is impairment of vestibular function with resulting vertigo symptoms. The incidence of this complication as reported in the literature varies widely from 0.33% to 75% [6].

Although numerous studies have reported the effects of CI on the vestibular function in deaf patients, there have been no reports examining the vestibular function in patients who had residual hearing at lower frequencies, or of the postoperative effects on vestibular function of new atraumatic concepts of electrode and surgical techniques.

We recently published a preliminary report that the round window approach (RWA) is preferable from the viewpoint of vestibular function [7].

The aim of the present study was to further examine the changes in vestibular functions after implantation in patients who underwent EAS CI.

Material and methods

Patients

Thirteen patients (four males and nine females) who underwent EAS CI in our center were included in this

Correspondence: Shin-ichi Usami, Department of Otolaryngology, Shinshu University School of Medicine, 3-1-1, Asahi, Matsumoto City, 390-8621, Japan. Tel: +81 263 37 2666. Fax: +81 263 36 9164. E-mail: usami@shinshu-u.ac.jp

(Received 11 May 2013; accepted 30 June 2013)

ISSN 0001-6489 print/ISSN 1651-2251 online © 2013 Informa Healthcare
DOI: 10.3109/00016489.2013.824110

study after obtaining informed written consent. The study was carried out with the approval of the Shinshu University Ethical Committee.

The age at implantation ranged from 30 to 60 years, and the mean age was 45.2 years. All patients fulfilled the following inclusion criteria: post-lingually acquired, bilateral sensorineural hearing loss (HL) with pure tone thresholds of <65 dB HL at the low frequencies (125, 250, and 500 Hz), of ≥80 dB HL at frequency 2 kHz, and of ≥85 dB HL at frequencies >4 kHz, and monosyllabic word recognition scores in quiet of ≤60% at 65 dB sound pressure level (SPL) in both ears in best-aided condition. Subjects were still included in this study if one of these frequencies was out of the mentioned decibel levels by only 10 dB or less.

Cochlear implantations

We performed CI with full insertion of the MED-DEL FLEX$^{EAS®}$ electrode (MED-EL, Innsbruck, Austria) in all patients.

All surgeries were performed by a single surgeon and the RWA was applied for electrode insertion. Systemic antibiotics and dexamethasone were administered peri- and postoperatively. Residual hearing was successfully preserved in all patients (data not shown).

Vestibular testing

The patients were examined by caloric testing and vestibular evoked myogenic potential (VEMP) before or after implantation, or both, to obtain data on semicircular canal function and otolithic function, respectively.

In VEMP testing, electromyography (EMG) was carried out using a pair of surface electrodes mounted on the upper half and the sterna head of the sternocleidomastoid (SCM) muscle. The electrographic signal was recorded using a Neuropack evoked potential recorder (Nihon Kohden Co. Ltd, Tokyo, Japan). Clicks lasting for 0.1 ms at 105 dBnHL were presented through a headphone. The stimulation rate was 5 Hz, the bandpass filter intensity was 20–2000 Hz, and analysis time was 50 ms. The responses to 200 stimuli were averaged twice. Because the amplitude of the VEMP based on the unrectified EMG is correlated with the activity of the SCM muscle during the test [8], we measured the activity of the SCM muscle using the background integrated EMG response, the area under the averaged rectified EMG curve, from –20 ms to 0 ms before the sound stimulation. The correction of the amplitude was calculated as follows [9]:

Corrected amplitude (ms^{-1}) = amplitude of the averaged unrectified EMG (micro V)/background integrated EMG (micro V ms)

In caloric testing, maximum slow phase velocity (SPV) was measured by cold water irrigation (20°C, 5 ml, 20 s). We defined below 10°/s of SPV as areflexia and between 10 and 20°/s as hyporeflexia.

Statistical analysis

SPSS for Windows software (Chicago, IL, USA) was used for all analyses, and paired t test was applied when comparing differences in preoperative and postoperative vestibular functions. Statistical significance was set at $p < 0.05$.

Results

The results are summarized in Table I.

Semicircular canal function

Preoperative evaluation was performed bilaterally. Three of 11 patients (27%, nos 3, 4, and 5) showed areflexia or hyporeflexia in caloric testing. Patient no. 4 had bilateral areflexia, no. 5 had implanted ear areflexia and non-implanted ear hyporeflexia, and no. 3, had hypoflexia only in the non-implanted ear.

Postoperative caloric testing was obtained after 1 month or more. All 13 patients underwent postoperative caloric testing and 11 of them were also examined before the EAS implantations. Two (nos 4 and 5) of 13 patients (15%) had abnormal postoperative caloric test results in the implanted ear, although both of them also had abnormal results before implantations. Figure 1 shows the caloric response before and after EAS implantations for the implanted ear. Compared with before implantations, the results after implantations were unchanged in all of the 11 patients who underwent both preoperative and postoperative testing. One patient (no. 4) had areflexia both before and after implantation. The mean SPV was 28.06°/s preoperatively (SD = 17.61) and 28.68°/s postoperatively (SD = 15.53). There were no significant differences between results before and after implantations in caloric testing ($p = 0.67$).

Otolithic function

When preoperative evaluation was performed, no patients showed absent response in VEMP.

Postoperative VEMP was obtained after 1 month or more. All 13 patients underwent postoperative VEMP and 11 of them were also examined before EAS implantations. No patient had absent VEMP response

Table I. Summary of patients' details.

Patient no.	Age (years)/sex	Implanted side	Caloric test (°/s)				VEMP (ms^{-1})			
			Implanted ear		Non-implanted ear		Implanted ear		Non-implanted ear	
			Preop	Postop	Preop	Postop	Preop	Postop	Preop	Postop
1	41/M	R	NA	22.28	NA	20.74	NA	0.060	NA	0.068
2	47/F	L	NA	24.41	NA	9.09†	NA	0.029	NA	0.022
3	40/F	L	22.67	24.65	17.61*	17.76*	0.055	0.053	0.041	0.061
4	60/F	R	0†	0†	6.05†	0†	0.017	0.012	0.029	0.022
5	46/F	R	4.46†	8.31†	15.14*	19.94*	0.012	0.015	0.024	0.025
6	39/F	L	52.84	50	46.26	38.76	0.027	0.023	0.028	0.047
7	47/F	R	26.64	28.2	22.18	27.31	0.020	0.018	0.024	0.022
8	30/M	R	29.62	39.65	31.1	14.69	0.062	0.032	0.045	0.028
9	40/M	L	24.94	29.39	38.11	23.4	0.026	0.019	0.046	0.025
10	35/F	L	23.18	22.91	22.24	21.96	0.025	0.026	0.030	0.040
11	52/M	R	22.57	22.02	22.44	22.98	0.018	0.020	0.023	0.017
12	51/F	L	52.57	45.97	50.26	54.95	0.036	0.033	0.041	0.026
13	59/F	L	49.18	43.44	54.3	43.44	0.010	0.008	0.038	0.024

NA, not available.
*Hyporeflexia.
†Areflexia.

in the implanted ear. Figure 2 shows corrected VEMP amplitudes before and after EAS implantations for the implanted ear. Although one (no. 8) of the 11 patients (9%) had a decreased response in corrected VEMP amplitude, corrected VEMP amplitudes after implantations were unchanged in all but one of the patients, when compared with preoperative results. The mean corrected amplitude was 0.028 preoperatively (SD = 0.017) and 0.023 postoperatively (SD = 0.013). There were no significant differences between results before and after implantation in VEMP testing ($p = 0.095$).

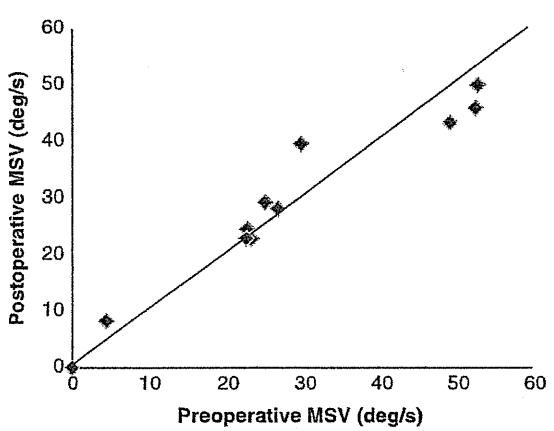

Figure 1. Results of caloric testing before and after EAS implantations in the implanted ear. There were no significant differences between preoperative and postoperative results ($p = 0.67$). MSV, maximum slow eye velocity.

Discussion

Previous reports showed that the frequencies of 'preoperative' vestibular disorders in profound hearing loss patients were about 30–73% in caloric testing [10–14] and about 11–65% in VEMP [10–15].

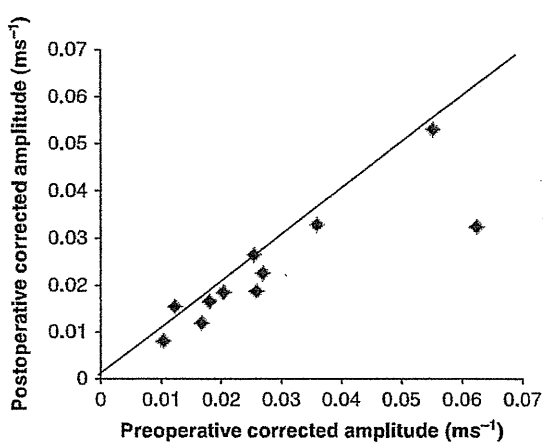

Figure 2. Results of VEMP before and after EAS implantations in the implanted ear. There were no significant differences between preoperative and postoperative results of VEMP testing in EAS implanted ears ($p = 0.095$). Corrected amplitude was used to compare the results.

In this study, we found that the 'preoperative' frequencies of vestibular disorders in hearing loss patients with residual hearing who received EAS were 27% and 0% in caloric testing and VEMP, respectively.

This finding suggested that vestibular function of the patients who underwent EAS was relatively good compared with the patients with profound hearing loss who underwent conventional CI.

In this study, to preserve such good vestibular function, atraumatic CI surgery (RWA with flexible thin electrode) was performed. Although one patient showed a decreased VEMP result, there was no hypofunction in postoperative caloric testing when compared with preoperative results in the implanted ear.

According to previous reports, various frequencies of postoperative deterioration in vestibular function were demonstrated. Postoperative hypofunction was found in 6–58% in the caloric testing [10–14,16–18], and 13–86% in VEMP [10–15]. One of the reasons for such variation is probably the surgical technique applied.

Todt et al. reported that hypofunction of postoperative VEMP was seen in 50% of patients who underwent cochleostomy and 13% of those with RWA Also, abnormal postoperative caloric testing results were seen in 42.9% of the patients who underwent cochleostomy and 9.4% of those who had the RWA [10].

Temporal bone studies have shown that an electrode insertion into the scala vestibuli involves damage of the osseous spiral lamina, basilar membrane, and vestibular receptors. The saccule was the most frequently damaged vestibular receptor, followed by the utricle and the semicircular canals [19].

However, when the electrode was inserted into the scala tympani, no vestibular damage was found [19]. Adunka et al. evaluated cochlear implant electrode insertions through the round window membrane histologically and reported that smooth implantations via round the window membrane resulted in deep, atraumatic insertions into the scala tympani [20]. Unintentional lesions to the basilar membrane can be avoided by using the round window as an exact anatomic landmark that is always in direct continuity with the scala tympani [20]. Previous histological and clinical studies clearly showed that the RWA is the technique that preserves the vestibular functions to the greatest extent and therefore is better than cochleostomy.

In the present study, the FLEX^{EAS} electrode was used for all of the patients. The cross-sectional diameter of the electrode is smaller than a conventional electrode, varying from 0.33 by 0.49 mm at the apex and to 0.8 mm at the basal, and a major feature of the device is its superior flexibility. Histology and dissection of human temporal bones performed by Adunka et al. confirmed the atraumatic character of this device [20]. Insertion forces with the conventional array and FLEX array were measured in an acrylic model of the scala tympani, demonstrating that insertion force could be reduced significantly by more than 40% with the FLEX^{EAS} electrode [4]. As in our previous study [7], such a smaller diameter and more flexible electrode might enable less damage to not only the cochlear tissue, but also the vestibular organs.

In conclusion, patients undergoing EAS implantation have good vestibular function compared with the vestibular function of the patients with profound hearing loss. It is important to preserve not only residual hearing but also the vestibular function of the implanted ears, using atraumatic surgical techniques. The RWA with soft electrode is preferable to decrease the risk of damage to vestibular function.

Acknowledgments

We thank A.C. Apple-Mathews for help in preparing the manuscript. This study was supported by a Health and Labour Sciences Research Grant for Comprehensive Research on Disability Health and Welfare from the Ministry of Health, Labour and Welfare of Japan (S.U.) and by a Grant-in-Aid for Scientific Research from the Ministry of Education, Science and Culture of Japan (S.U.).

Declaration of interest: The authors report no conflicts of interest. The authors alone are responsible for the content and writing of the paper.

References

[1] von Ilberg CA, Baumann U, Kiefer J, Tillein J, Adunka OF. Electric-acoustic stimulation of the auditory system: a review of the first decade. Audiol Neurootol 2011;16:1–30.

[2] Lehnhardt E, Laszig R. 1994. Specific surgical aspects of cochlear implant soft surgery. In Hochmair-Desoyer IJ, Hochmair ES, editors. Advances in cochlear implants. Vienna: Manz. p. 228–9.

[3] Skarzynski H, Lorens A, Piotrowska A, Anderson I. Preservation of low frequency hearing in partial deafness CI (PDCI) using the round window surgical approach. Acta Otolaryngol 2007;127:41–8.

[4] Adunka O, Kiefer J, Unkelbach MH, Lehnert T, Gstoettner W. Development and evaluation of an improved cochlear implant electrode design for electric acoustic stimulation. Laryngoscope 2004;114:1237–41.

[5] Baumgartner WD, Jappel A, Morera C, Gstöttner W, Müller J, Kiefer J, et al. Outcomes in adults implanted with the FLEXsoft electrode. Acta Otolaryngol 2007;127: 579–86.

[6] Buchman CA, Joy J, Hodges A, Telischi FF, Balkany TJ, Vestibular effects of CI. Laryngoscope 2004;114:1–22.
[7] Usami S, Moteki H, Suzuki N, Fukuoka H, Miyagawa M, Nishio SY, et al. Achievement of hearing preservation in the presence of an electrode covering the residual hearing region. Acta Otolaryngol 2011;131:405–12.
[8] Colebatch JG, Halmagyi GM, Skuse NF. Myogenic potentials generated by a click-evoked vestibulocollic reflex. J Neurol Neurosurg Psychiatry 1994;57:190–7.
[9] Shojaku H, Takemori S, Kobayashi K, Watanabe Y. Clinical usefulness of glycerol vestibular-evoked myogenic potentials: preliminary report. Acta Otolaryngol Suppl 2001;545:65–8.
[10] Todt I, Basta D, Ernst A. Does the surgical approach in cochlear implantation influence the occurrence of postoperative vertigo? Otolaryngol Head Neck Surg 2008;138:8–12.
[11] Melvin TA, Della Santina CC, Carey JP, Migliaccio AA. The effects of cochlear implantation on vestibular function. Otol Neurotol 2009;30:87–94.
[12] Krause E, Louza JP, Wechtenbruch J, Gürkov R. Influence of cochlear implantation on peripheral vestibular receptor function. Otolaryngol Head Neck Surg 2010;142:809–13.
[13] Krause E, Wechtenbruch J, Rader T, Gürkov R. Influence of cochlear implantation on sacculus function. Otolaryngol Head Neck Surg 2009;140:108–13.
[14] Wagner JH, Basta D, Wagner F, Seidl RO, Ernst A, Todt I. Vestibular and taste disorders after bilateral cochlear implantation. Eur Arch Otorhinolaryngol 2010;267:1849–54.
[15] Licameli G, Zhou G, Kenna MA. Disturbance of vestibular function attributable to cochlear implantation in children. Laryngoscope 2009;119:740–5.
[16] Krause E, Louza JP, Hempel JM, Wechtenbruch J, Rader T, Gürkov R. Effect of cochlear implantation on horizontal semicircular canal function. Eur Arch Otorhinolaryngol 2009;266:811–17.
[17] Fina M, Skinner M, Goebel JA, Piccirillo JF, Neely JG, Black O. Vestibular dysfunction after cochlear implantation. Otol Neurotol 2003;24:234–42.
[18] Enticott JC, Tari S, Koh SM, Dowell RC, O'Leary SJ. Cochlear implant and vestibular function. Otol Neurotol 2006;27:824–30.
[19] Tien HC, Linthicum FH Jr. Histopathologic changes in the vestibule after cochlear implantation. Otolaryngol Head Neck Surg 2002;127:260–4.
[20] Adunka O, Unkelbach MH, Mack M, Hambek M, Gstoettner W, Kiefer J. Cochlear implantation via the round window membrane minimizes damage to cochlear structures: a histologically controlled insertion study. Acta Otolaryngol 2004;124:807–12.

Massively Parallel DNA Sequencing Successfully Identifies New Causative Mutations in Deafness Genes in Patients with Cochlear Implantation and EAS

Maiko Miyagawa[1], Shin-ya Nishio[1], Takuo Ikeda[2], Kunihiro Fukushima[3], Shin-ichi Usami[1]*

1 Department of Otorhinolaryngology, Shinshu University School of Medicine, Matsumoto, Japan, **2** Department of Otolaryngology, Tsudumigaura Handicapped Children's Hospital, Shunan, Japan, **3** Department of Otorhinolaryngology, Okayama University School of Medicine, Okayama, Japan

Abstract

Genetic factors, the most common etiology in severe to profound hearing loss, are one of the key determinants of Cochlear Implantation (CI) and Electric Acoustic Stimulation (EAS) outcomes. Satisfactory auditory performance after receiving a CI/EAS in patients with certain deafness gene mutations indicates that genetic testing would be helpful in predicting CI/EAS outcomes and deciding treatment choices. However, because of the extreme genetic heterogeneity of deafness, clinical application of genetic information still entails difficulties. Target exon sequencing using massively parallel DNA sequencing is a new powerful strategy to discover rare causative genes in Mendelian disorders such as deafness. We used massive sequencing of the exons of 58 target candidate genes to analyze 8 (4 early-onset, 4 late-onset) Japanese CI/EAS patients, who did not have mutations in commonly found genes including *GJB2*, *SLC26A4*, or mitochondrial 1555A>G or 3243A>G mutations. We successfully identified four rare causative mutations in the *MYO15A*, *TECTA*, *TMPRSS3*, and *ACTG1* genes in four patients who showed relatively good auditory performance with CI including EAS, suggesting that genetic testing may be able to predict the performance after implantation.

Citation: Miyagawa M, Nishio S-y, Ikeda T, Fukushima K, Usami S-i (2013) Massively Parallel DNA Sequencing Successfully Identifies New Causative Mutations in Deafness Genes in Patients with Cochlear Implantation and EAS. PLoS ONE 8(10): e75793. doi:10.1371/journal.pone.0075793

Editor: Akinori Kimura, Tokyo Medical and Dental University, Japan

Received July 16, 2013; **Accepted** August 21, 2013; **Published** October 9, 2013

Funding: This study was supported by a Health and Labour Sciences Research Grant for Comprehensive Research on Disability Health and Welfare from the Ministry of Health, Labour and Welfare of Japan (http://www.mhlw.go.jp/english/) (S.U.), and by a Grant-in-Aid for Scientific Research from the Ministry of Education, Science and Culture of Japan (http://www.mext.go.jp/english/) (S.U.). The funders had no role in study design, data collection and analysis, decision to publish, or preparation of the manuscript.

Competing Interests: All authors declare no competing interests.

* E-mail: usami@shinshu-u.ac.jp

Introduction

Cochlear Implantation (CI) has been established as a standardized therapy for severe to profound hearing loss [1]. Electric Acoustic Stimulation (EAS) is a hearing implant system combining a cochlear implant and acoustic amplification technology in one device, and has recently become a standard intervention for the patients with partial deafness, defined as a mild to moderate low-frequency sensorineural hearing loss sloping to a profound hearing loss in the higher frequencies [1]. One difficult point is that outcomes of CI/EAS are variable and many factors are thought to be involved in post-implantation performance. Satisfactory auditory performance in the patients with various deafness gene mutations indicates that genetic background would be helpful in predicting performance after CI [2]. When genetic background is involved in intra-cochlear etiology, there is potential for good performance. Therefore, it is important to identify the involved region inside/outside of the cochlea by identifying the responsible gene. Decisions as to whether to undergo EAS surgery and the timing of the surgery, as well as prediction of outcome after EAS is sometimes difficult because of individual differences in progression, which is sometimes of a rather rapid nature but sometimes rather stable. One advantage of genetic testing is that the possible prognosis for hearing, i.e., progressive or not, can be predicted for individual patients.

Etiological studies have shown genetic disorders to be a common cause of deafness, but difficulty lies in the fact that deafness is an extremely heterogenous disorder.

Invader-based multi-gene screening for 13 genes/46 mutations commonly found in Japanese, identified the responsible mutations in approximately 30% of deafness patients [3], accelerating the clinical application of gene screening. However, the etiology of the rest of the patients is still unknown. In addition, the involvement of at least 58 distinct genes sometimes makes the precise diagnosis difficult.

Targeted exon sequencing of selected genes using the Massively Parallel DNA Sequencing (MPS) technology will potentially enable us to systematically tackle previously intractable monogenic disorders and improve molecular diagnosis. We have recently reported that target exon sequencing using MPS is a powerful tool to identify rare gene mutations for deafness patients [4].

In this study, we have chosen 58 deafness-causative genes, and conducted genetic analysis using MPS-based genetic screening to find the rare genes responsible for the patients who received CI or EAS.